STIC-ILL

Ql. N2
+
MIC

From: Gambel, Phillip
Sent: Tuesday, December 05, 2000 8:16 AM
To: STIC-ILL
Subject: springer and icam

stic

please provdie the following references to

phillip gambel
art unit 1644
308-3997

1644 mailbox 9E12

1. rothlein et al. j. immunol. 137 / 4 : 1270 - 1274 (1986)
PLEASE COPY THE FRONT COVER OF THE JOURNAL SO I CAN DETERMINE MONTH OF PUBLICATION .
THANX

2. dustin et al. j. immunol. 137 / 1 : 245 - 254 (1986)
PLEASE COPY THE FRONT COVER OF THE JOURNAL SO I CAN DETERMINE MONTH OF PUBLICATION .
THANX

3. staunton et al. cell 52 / 6 : 925 - 933/934 (1988)
PLEASE COPY THE FRONT COVER OF THE JOURNAL SO I CAN DETERMINE MONTH OF PUBLICATION .
THANX

4.martin et al. cell 53 / 5 : 813 - 819 (1988)
PLEASE COPY THE FRONT COVER OF THE JOURNAL SO I CAN DETERMINE MONTH OF PUBLICATION .
THANX

5. simmons et al. nature 331 / 6157 : 624 - 627 (1988)
PLEASE COPY THE FRONT COVER OF THE JOURNAL SO I CAN DETERMINE MONTH OF PUBLICATION .
THANX

nature

INTERNATIONAL WEEKLY JOURNAL OF SCIENCE

331 No.6151 7 January 1988 £4.95

Publication Date

Q1
12

FIRE FOUNTAINS

Table 1 Percentage of intercalated cells in cortical collecting duct showing apical, basolateral or diffuse staining for H^+-ATPase

Animal	Antibody	Staining pattern		
		Apical	Basolateral	Diffuse
1 (86)	70K	31	9	60
2 (151)	70K	40	12	48
3 (77)	70K	44	38	18
4 (131)	56K	42	13	45
5 (127)	56K	39	7	54
6 (89)	56K	30	52	18
7 (150)	31K	49	15	36
8 (63)	31K	35	54	11
9 (78)	31K	50	6	44

Numbers in parentheses indicate the number of cells counted to derive each percentage. Cells were counted on sections immunostained by the ABC-peroxidase procedure (Vector, Burlinghame, California).

42% ($n = 3,927$); inner medulla (initial part), 13% ($n = 1,965$). These figures are consistent with previous estimations of the prevalence of intercalated cells in each collecting-duct segment; the values were similar with all three antibodies. In addition, we quantified the percentage of intercalated cells with the three distinct labelling patterns in cortical collecting ducts from different animals (Table 1). The proportion of cells with basolateral and diffuse staining appeared to be inversely related, and varied considerably among animals, whereas the percentage of cells with marked apical staining was less variable. These findings suggest that redistribution of proton pumps from a diffuse to a basolateral location may occur, whereas the population of cells with apical pumps is more stable. They do not exclude, however, a relocation of proton pumps from basolateral to apical plasma membranes, or vice versa.

Our results provide the first direct evidence in support of models of bicarbonate secretion by the cortical collecting tubule, in which proton pumps located basolaterally are believed to generate intracellular bicarbonate that exits at the apical plasma membrane[1,3,18]. The heavy apical staining of all intercalated cells in the inner stripe of the outer medulla is consistent with physiological data showing that this segment has the highest rate of transepithelial proton secretion in the kidney[19].

What are the mechanisms that enable the cortical intercalated cells to direct proton pumps to either the apical or basolateral plasma membrane, or to intracellular vesicular compartments? One possibility is that proton pumps destined for the different membrane domains have alternative structures that provide targetting information. Our studies demonstrate that apical and basolateral pumps are immunologically similar, but more investigation will be necessary to determine whether subtle structural differences are present among pumps in different membrane compartments. Indeed, preliminary evidence does suggest that both the 56K (ref. 9) and 31K subunits may have isoforms (S.H. *et al.*, unpublished data). Alternatively, factors other than enzyme structure may determine cellular destination. It has been suggested[20,21] that the internal pH of transport vesicles can determine their polarity of fusion, but both apical and basolaterally directed vesicles appear to be highly acidic in intercalated cells[3]. The microtubular system could also be involved in sorting processes. A viral haemagglutinin is mis-directed after colchicine treatment of MDCK cells[22], and microtubule disruption prevents the rapid, CO_2-induced insertion of H^+-ATPase into the apical membrane of proton-secreting cells[16,17]; whether microtubules can regulate the polarity of proton pump insertion remains to be investigated. In conclusion, our data provide a unique example of adjacent epithelial cells with opposing polarities with respect to a major transporting enzyme. These cells represent an intriguing system in which factors that are involved in the specific targetting and insertion of membrane proteins can be examined.

This project was supported by the NIH, the National Kidney Foundation (S.H.) and the Searle Scholars' Program (S.G.). D.B. is an Established Investigator of the American Heart Association and received partial support from a Chugai Fellowship and a grant from the Milton Fund. We thank Betty Ytzaina for secretarial help and Joanne Natale for excellent technical assistance.

Received 30 November 1987; accepted 12 January 1988.

1. Steinmetz, P. R. *Am. J. Physiol.* **251**, F173-F187 (1986).
2. Kelly, R. B. *Nature* **326**, 14-15 (1987).
3. Schwartz, G. J., Barasch, J. & Al-Awqati, Q. *Nature* **318**, 368-371 (1985).
4. Drenckhahn, D., Schluter, K., Allen, D. P. & Bennett, V. *Science* **230**, 1287-1289 (1985).
5. Schuster, V. L., Bonsib, S. M. & Jennings, M. L. *Am. J. Physiol.* **251**, C347-C355 (1986).
6. McLean, I. W. & Nakane, P. K. *J. Histochem. Cytochem.* **22**, 1077-1083 (1974).
7. Altman, L. G., Schneider, B. G. & Papermaster, D. S. *J. Histochem. Cytochem.* **32**, 1217-1223 (1984).
8. Maxwell, M. H. *J. Microsc.* **112**, 253-255 (1978).
9. Gluck, S. & Caldwell, J. *J. biol. Chem.* (in the press).
10. Brown, D., Gluck, S. & Hartwig, J. H. *J. Cell Biol.* **105**, 1637-1648 (1987).
11. Roth, J., Bendayan, M. & Orci, L. *J. Histochem. Cytochem.* **26**, 1074-1081 (1978).
12. Brown, D. & Orci, L. *Am. J. Physiol.* **250**, C605-C608 (1986).
13. Madsen, K. M. & Tisher, C. C. *Am. J. Physiol.* **245**, F670-F679 (1983).
14. Brown, D., Weyer, P. & Orci, L. *Anat. Rec.* **218**, 237-242 (1987).
15. Schwartz, G. J. & Al-Awqati, Q. *J. clin. Invest.* **75**, 1638-1644 (1985).
16. Stetson, D. L. & Steinmetz, P. R. *Am. J. Physiol.* **245**, C113-C120 (1983).
17. Gluck, S., Cannon, C. & Al-Awqati, Q. *Proc. natl. Acad. Sci. U.S.A.* **79**, 4327-4331 (1982).
18. Stetson, D. L. & Steinmetz, P. R. *Am. J. Physiol* **249**, F553-F565 (1985).
19. Lombard, W. E., Kokko, J. P. & Jacobson, H. R. *Am. J. Physiol.* **244**, F289-F296 (1983).
20. Orci, L., Ravazzola, M. & Anderson, R. G. W. *Nature* **326**, 77-79 (1987).
21. Caplan, M. J. *et al. Nature* **329**, 632-635 (1987).
22. Rindler, M. J., Ivanov, I. E. & Sabatini, D. D. *J. Cell Biol.* **104**, 231-241 (1987).
23. Towbin, M., Staehelin, T. & Gordon, J. *Proc. natl. Acad. Sci. U.S.A.* **76**, 4350-4354 (1979).
24. Slot, J. W. & Geuze, H. J. *Eur. J. Cell Biol.* **38**, 87-93 (1985).

ICAM, an adhesion ligand of LFA-1, is homologous to the neural cell adhesion molecule NCAM

David Simmons, Malegapuru W. Makgoba* & Brian Seed

Department of Molecular Biology and Department of Genetics, Harvard Medical School, Massachusetts General Hospital, Boston, Massachusetts, 02114, USA
* Immunology Branch, National Cancer Institute, National Institutes of Health, Bethesda, Maryland 02115, USA

Antigen-specific cell contacts in the immune system are strengthened by antigen-nonspecific interactions, mediated in part by lymphocyte-function associated (LFA) antigens[1,2]. The LFA-1 antigen is widely expressed on cells of haematopoietic origin and is a major receptor of T cells, B cells and granulocytes[3]. LFA-1 mediates the leukocyte adhesion reactions underlying cytolytic conjugate formation, helper T-cell interactions, and antibody-dependent killing by natural killer cells and granulocytes. Recently, ICAM-1 (intercellular adhesion molecule-1) has been defined as a ligand for LFA-1[4-6]. Monoclonal antibodies to ICAM-1 block T lymphocyte adhesion to fibroblasts and endothelial cells and disrupt the interaction between cytotoxic T cells and target cells. In addition, purified ICAM-1 reconstituted into artificial membranes binds LFA-1$^+$ cells[6]. ICAM-1 is found on leukocytes, fibroblasts, epithelial cells and endothelial cells and its expression is regulated by inflammatory cytokines. LFA-1 has been placed in the integrin family of cell surface receptors by virtue of the high sequence similarity between the LFA-1 and integrin β chains[7,8]. The adhesion ligands of the integrin family are glycoproteins bearing the Arg-Gly-Asp (RGD) sequence motif, for example, fibronectin, fibrinogen, vitronectin and von Willebrand factor[9]. Here we show that a complementary DNA clone ICAM-1 contains no RGD motifs, but instead is homologous to the neural cell adhesion molecule NCAM[10,11].

A cDNA library was constructed using RNA prepared from HL-60 cells induced with 12-*O*-tetradecanoyl phorbol 13-acetate

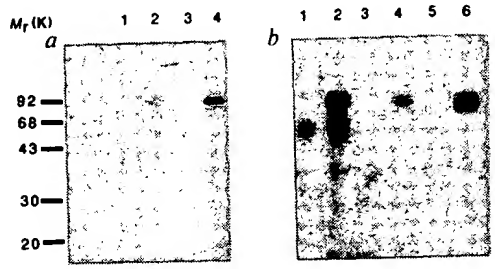

Fig. 1 Immunoprecipitation of ICAM-1 from ^{125}I-surface-labelled cells, using mAb 84H10. *a*, Mock-transfected (lane 1) and pICAM-1-transfected (lane 2) COS cells. Uninduced (lane 3), and TPA-stimulated (lane 4) HL-60 cells. *b*, Regulation of ICAM-1 synthesis in HL-60 cells by cytokines. Lane 1, γ-IFN-induced, without antibody; lane 2, γ-IFN-induced, with antibody; lane 3, TNF-induced, without antibody; lane 4, TNF induced, with antibody; lane 5, IL-1β induced, without antibody; lane 6, IL-1β induced, with antibody. COS cells were transfected with pICAM-1 as previously described[12]. HL-60 cells were maintained at 5×10^5 ml^{-1} and test reagents added for 48 h at the following concentrations; 50 ng ml^{-1} TPA, 100 U ml^{-1} γ-IFN, 200 U ml^{-1} TNF and 10 U ml^{-1} IL-1β.

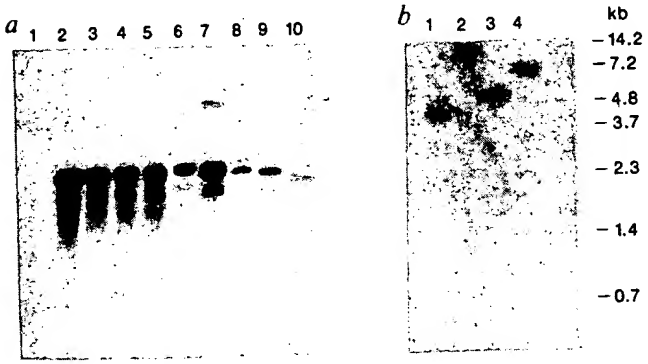

Fig. 2 Expression and structure of ICAM-1 gene. *a*, RNA blot hybridization. Total RNA (20 μg) was denatured in formaldehyde, electrophoresed, transferred to nylon membranes and hybridized with ICAM-1 cDNA. Lane 1, uninduced HL-60; lane 2, TPA-induced HL-60; lane 3, γ-IFN-induced HL-60; lane 4, IL-1β-induced HL-60; lane 5, TNF-induced HL-60; lane 6, JY (lymphoblastoid cell line); lane 7, Raji (Burkitt's lymphoma); lane 8, Peer (T cell leukaemia); lane 9, T blasts; lane 10, LAK cells. The 1.9kb species is partially occluded by the 18S rRNA. Stimulation of HL-60 cells was the same as in Fig. 1. T-cell blasts were obtained by culture of peripheral blood lymphocytes with phytohaemagglutinin for 48 h. *b*, Genomic DNA blot hybridization. Human placenta genomic DNA (20 μg) was digested with restriction enzymes, electrophoresed, transferred to nylon membranes and hybridized with ICAM cDNA. Lane 1, *Eco*RI; lane 2, *Bam*HI; lane 3, *Hin*dIII; lane 4, *Dra*I.

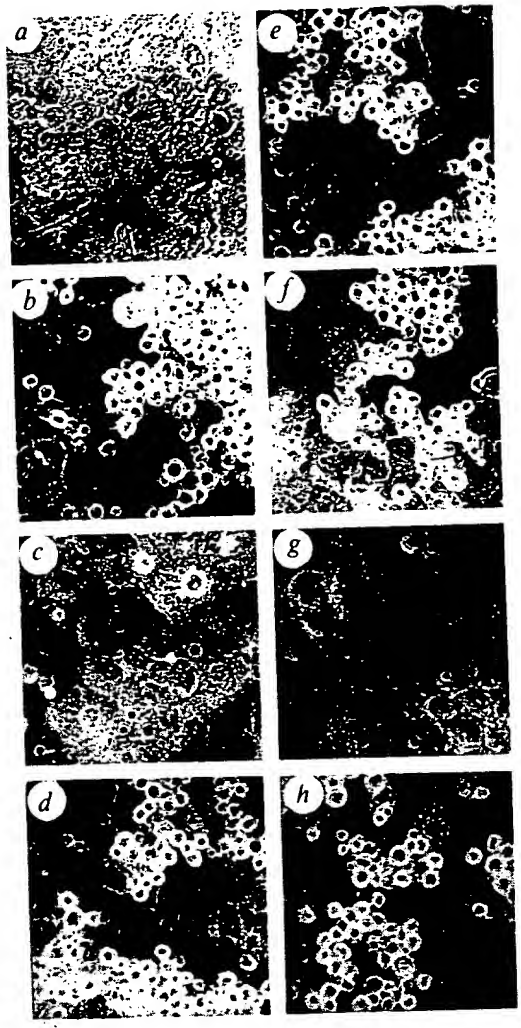

Fig. 3 Functional analysis of pICAM-1. COS cells were transfected with control vector πH3M or pICAM-1 cDNA and HL-60 cell adhesion assays performed 48 h later. *a*, COS cells transfected with vector only; *b–h*, COS cells transfected with pICAM-1 and treated as indicated. *b*, no antibodies present; *c*, anti-ICAM antibody on COS cells; *d*, control anti-HLA antibody on COS cells; *e*, anti-ICAM antibody on HL-60 cells; *f*, anti-HLA antibody on HL-60 cells; *g*, anti-LFA-1 antibodies on HL-60 cells; *h*, anti-LFA-1antibodies on COS cells. COS cells or HL-60 cells were preincubated with the stated antibodies at 1 μg ml^{-1} for 1 h at 4 °C in PBS/5% fetal bovine serum. In *c*, the anti-ICAM-1 antibody (84H10) was washed off the COS cells to prevent the excess from binding the HL-60 cells. In all other cases the antibodies were left in contact with the cells to prevent leaching. The HL-60 cells were allowed to adhere to the COS cells for 30 min at 37 °C in medium containing 10 mM Mg^{2+}, washed 3 times and photographed.

(TPA). The library was transfected into COS cells and cells expressing surface antigens were recovered by panning with the anti-ICAM monoclonal antibodies (mABs) 8F5 and 84H10 (ref. 12). Episomal DNA was recovered from the panned cells and the expression-panning cycle[13,14] repeated twice to obtain a cDNA clone designated pICAM-1.

COS cells transfected with pICAM-1 gave positive surface immunofluorescence reactions with three anti-ICAM-1 antibodies; 8F5 and 84H10 (data not shown), and RR-1 (N. Hogg, personal communication). Immunoprecipitation of pICAM-1 transfected COS cells with 84H10 antibody gave a band of relative molecular mass (M_r) 100,000 (100K, Fig. 1). A slightly larger protein (110K) was precipitated from HL-60 cells induced for 48 h with either TPA, γ-interferon (γ-IFN), tumour necrosis factor (TNF), or interleukin-1β (IL-1β), but was absent from uninduced cells (Fig. 1). The smaller molecular mass of ICAM-1 expressed in COS cells is consistent with the reduced molecular masses observed for other surface antigens expressed in COS cells[13,14].

RNA blot analysis (Fig. 2a) showed two species of 3.2 kilobases (kb) and 1.9 kb present in HL-60 cells stimulated with either TPA, γ-IFN, TNF or IL-1β, but absent in uninduced cells. The 1.9-kb band is occluded by the 18S ribosomal RNA but is present as a distinct species in poly(A)$^+$ RNA (data not shown). Thus, the expression of ICAM-1 is regulated by a number of inflammatory cytokines, apparently at the transcription level. Similar species were present in B cells (JY and Raji), and T cells (Peer and T blasts). A slightly smaller transcript was

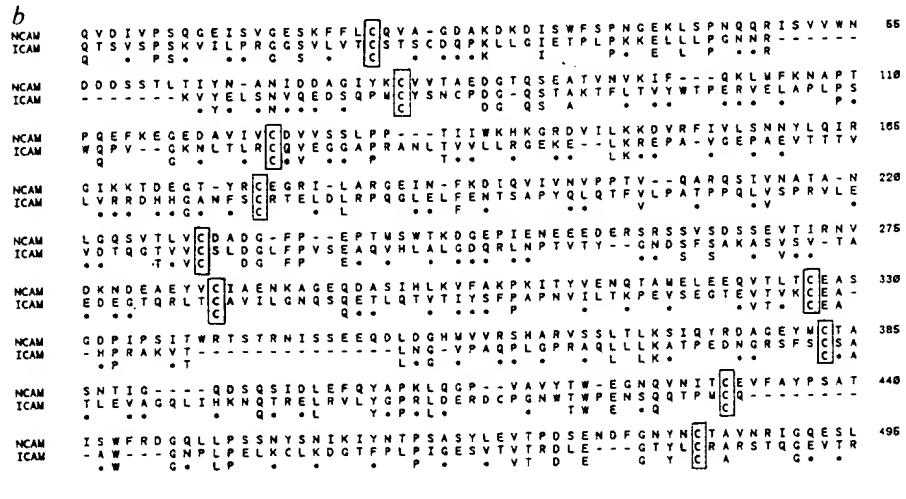

Fig. 4 Sequence of ICAM-1 and homology with NCAM-1, *a*, Complete nucleotide sequence of ICAM-1 cDNA insert and predicted protein sequence. Nucleotide numbering is at right, amino acid numbering in parentheses at left. The RGE motif at position 152 is underlined, the potential *N*-linked glycosylation sites are indicated by -CHO-, and the transmembrane domain by -TM-. The amino acid sequence is numbered from the projected cleavage site of the signal peptide. Sequencing was by dideoxy-chain termination[20], using a combination of subclones and specific oligonucleotides. *b*, Homology with NCAM-1. Alignment of ICAM-1 with murine NCAM-1 (ref. 11) produced by the ALIGN program of the Protein Identification Resource (NBRF) (ref. 16). Residues beneath the aligned sequence indicate identity; asterisks indicate the residues are closely related, using the Dayhoff scoring matrix. Conserved cysteine residues are boxed.

detected in lymphokine-activated killer (LAK) cells. The structure of these ICAM-1 transcripts and their relationship to the pICAM-1 cDNA remains to be established. Blot hybridization of genomic DNA from placenta revealed a pattern consistent with a single-copy gene (Fig. 2*b*).

To investigate whether pICAM-1 encodes a functional cell adhesion molecule, COS cells expressing ICAM-1 were tested for their ability to bind HL-60 cells. After 30 minutes at 37 °C in the presence of Mg^{2+}, HL-60 cells strongly adhered to the ICAM-1-expressing COS cells, but not to mock-transfected cells (Fig. 3*a*, *b*). The specificity of this adhesion was demonstrated by preincubating the ICAM-1-expressing COS cells with 84H10 antibody. All HL-60 binding was abolished under these conditions (Fig. 3*c*). An isotype-matched monoclonal antibody, W6/32, which recognizes a monomorphic HLA-ABC related determinant of roughly equal abundance to ICAM-1 on transfected COS cells, had no effect on the adhesion (Fig. 3*d*). Similarly, preincubation of the HL-60 cells with either 84H10 or W6/32 did not inhibit binding (Fig. 3*e*, *f*). To determine if LFA-1 was acting as the receptor for ICAM-1 in this system, HL-60 cells were pretreated with antibodies against the β chain of LFA-1 (CD18; ref. 12) and subjected to the binding assay. All adhesion to ICAM-expressing COS cells was blocked (Fig. 3*g*). Pretreatment of COS cells with the CD18 antibodies had no effect on the adhesion (Fig. 3*h*). This provides direct evidence that ICAM-1 acts as an adhesion ligand for LFA-1.

The sequence of the pICAM-1 cDNA insert consists of 1,846 nucleotides (Fig. 4*a*). The predicted peptide sequence of 532 residues has the typical features of a transmembrane protein, including a putative signal sequence, which may be cleaved between glycine 25 and asparagine 26 (ref. 15), and a single 25-residue membrane-spanning domain terminating in a short, highly-charged cytoplasmic domain. The extracellular domain contains seven potential *N*-linked glycosylation sites which could adequately explain the difference in size between the deglycosylated precursor (55K) and the final product (90–115K) (ref. 5). Differential use of these putative glycosylation sites could also explain the heterogeneous molecular mass of ICAM-1 observed in different cell types[5].

LFA-1 is a member of the integrin family of cell-surface receptors[7,8]. The tripeptide motif Arg-Gly-Asp is a common feature of the ligands for this family and is required for ligand-

receptor interaction[9]. But ICAM-1 contains no RGD motifs, bearing instead a single RGE sequence at position 152. A search of the National Biomedical Research Foundation[16] (NBRF) database revealed no significant similarities to other proteins. Comparison with a laboratory database containing recently published surface proteins, however, did reveal a surprising and significant similarity between ICAM-1 and the neural cell adhesion molecule NCAM-1 (refs 10, 11; Fig. 4*b*). The optimal alignment score obtained using the NBRF ALIGN program is eight standard deviations above the mean score obtained from 500 random permutations of the sequences. The probability of the spontaneous occurrence of an equal or higher score is $\sim 10^{-9}$. Using a database of known immunoglobulin-related sequences it has been shown that ICAM-1 may be divided into five domains (28–112, 115–206, 217–310, 312–391, and 399–477), each of which shows significant similarity with other members of the immunoglobulin superfamily[17] (A. F. Williams, personal communication). For example, domain I is similar to CD3, whereas domains IV and V are similar to domains of myelin-associated glycoprotein[18] and carcinoembryonic antigen[19]. All five domains of NCAM align with the domains in ICAM-1 (Fig. 4*b*), and the principal contribution to the similarity comes from domains II and III of ICAM-1. Finally, the T-cell-specific adhesion molecule CD2 shows roughly the same similarity to NCAM as does ICAM, but ICAM and CD2 are only weakly related (not shown). Thus, some precursor of NCAM is ancestral to both ICAM and CD2.

The similarity of ICAM and NCAM is particularly interesting as it brings together lymphoid and neuronal adhesion molecules. In addition, it is surprising that ICAM is immunoglobulin-related, as its receptor LFA-1 is not. The LFA-1/ICAM-1 pairing demonstrates the interaction of two distinct molecular families, the immunoglobulin family and the integrin family. The availability of a functional ICAM-1 cDNA will allow a better assessment of the importance of ICAM-1/LFA-1-mediated adhesion in antigen-specific leukocyte function, including T-cell mediated killing, T-helper responses and antibody-dependent cell-mediated killing.

We thank Andrew J. McMichael for the myeloid panel of antibodies from the Third International Workshop on Leukocyte Typing, Alan F. Williams for detailed comparison of ICAM with the immunoglobulin superfamily, Nancy Hogg for cytometric analysis of ICAM-1 transfected COS cells and information about mAbs 8F5 and 84H10, Michael Bevilacqua for suggesting the use of HL-60 cells in the adhesion assays and for IL-1 and TNF, Ivan Stamenkovic for B-cell RNAs, and Mike Cherry and Jennifer Doudna for oligonucleotides. This work was supported by a grant from Hoechst AG.

Received 15 October; accepted 22 December 1987.

1. Springer, T. A., Dustin, M. L. Kishimoto, T. K. & Marlin, S. D. *A. Rev. Immun.* **5**, 223–252 (1987).
2. Anderson, D. C. & Springer, T. A. *Rev. Med.* **5**, 175–194 (1987).
3. Rothlein, R. & Springer, T. A. *J. exp. Med.* **163**, 1132–1149 (1987).
4. Rothlein, R., Dustin, M. L., Marlin, S. D. & Springer, T. A. *J. Immun.* **137**, 1270–1275 (1986).
5. Dustin, M. L., Rothlein, R., Bahn, A. K., Dinarello, C. A. & Springer T. A. *J. Immun.* **137** 245–254 (1986).
6. Marlin, S. D. & Springer, T. A. *Cell* **51**, 813–819 (1987).
7. Kishimoto, T. K., O'Conner, K., Lee, A., Roberts, T. M. & Springer, T. A. *Cell* **48**, 681–690 (1987).
8. Hynes, R. O. *Cell* **48**, 549–554 (1987).
9. Ruoslahti, E. & Pierschbacher, M. D. *Cell* **44**, 517–518 (1987).
10. Cunningham, B. A. *et al. Science* **236**, 799–806 (1987).
11. Barthels, D. *et al. EMBO J.* **6**, 907–914 (1987).
12. *Leukocyte Typing III. White Cell Differentiation Antigens* (eds McMichael, A. J. *et al.*) (Oxford University Press, 1987).
13. Seed, B. & Aruffo, A. *Proc. natn. Acad. Sci. U.S.A.* **84**, 3365–3369 (1987).
14. Aruffo, A. & Seed, B. *Proc. natn. Acad. Sci. U.S.A.* **84**, 8573–8577 (1987).
15. von Heijne, G. *Nucleic Acids Res.* **14**, 4683–4690 (1986).
16. Dayhoff, M. O., Barker, W. C. & Hunt, L. T. *Meth. Enzym.* **91**, 524–545 (1983).
17. Williams, A. F. *Immun. Today* **8**, 298–303 (1987).
18. Arguint, M. *et al. Proc. natn. Acad. Sci. U.S.A.* **84**, 600–604 (1987).
19. Beauchemin, N., Benchimol, S., Cournoyer, D., Fuks, A. & Stanners, C. P. *Molec. cell. Biol.* **7**, 3221–3230 (1987).
20. Sanger, F., Nicklen, S. & Coulson, A. R. *Proc. natn. Acad. Sci. U.S.A.* **74**, 5463–5467 (1977).

The adult T-cell receptor δ-chain is diverse and distinct from that of fetal thymocytes

John Francis Elli tt*, Edwin P. Rock*, Phillip A. Patten†, Mark M. Davis*† & Yueh-hsiu Chien*

* Departments of Medical Microbiology and † Biology, and † Howard Hughes Medical Institute, Stanford University, Stanford, California 94305, USA

T lymphocytes recognize foreign molecules using the T-cell receptor (TCR), a disulphide-linked heterodimer closely associated with the CD3 polypeptide complex on the cell surface. The TCR αβ heterodimers seem largely responsible for the recognition properties of both helper (T_H) and cytotoxic (T_C) T cells[1,2]. Recently, a second CD3-associated T-cell receptor heterodimer, γδ, has been described[3–9]. Cells bearing the γδ receptor appear before those bearing αβ during thymic ontogeny[8,9] and persist as a minor component (1–10%) of mature peripheral T cells. Their function is unknown. As there are a limited number of functional TCR V_γ gene segments[10], the size and potential diversity of the V_δ repertoire is important for the number of different antigens that may be recognized by γδ heterodimers. The δ-chain locus is located 75 kilobases (kb) 5′ to the TCR C_α coding region[11,12], raising the possibility that the α and δ *V*-region repertoires may overlap. Also, analysis of rearrangements at the δ-chain locus in developing thymocytes shows distinct fetal and adult patterns[11] indicating that there may be differences between the fetal and adult V_δ repertoires. To address these questions, we have characterized a large number of δ-containing complementary DNA clones from adult double-negative thymocytes ($CD4^-8^-$), an immature population that is enriched for γδ-bearing cells[5]. We find that a limited number of V_δ sequences are used, showing little overlap with known adult V_αs and differing significantly from fetal V_δs. But as two *D* elements may participate simultaneously in V_δ gene assembly, and random nucleotides may be added at any one of three junctional points, the potential number of different δ chains that can be made in the adult thymus is very large ($\sim 10^{13}$).

Complementary DNA libraries were constructed using RNA from adult double-negative ($CD4^-8^-$) thymocytes (DN thymocytes). Of the 129 δ-cDNA clones, 53 contained the first domain of C_δ, and 17 of these were sequenced. Ten contain all or part of a *V* region (Fig. 1*a*), and these are divided into leader (*L*), variable (*V*), diversity (*D*), and joining (*J*) regions by comparison with the published V_δ, V_α, $D_{\delta1}$, $D_{\delta2}$, $J_{\delta1}$ and $J_{\delta2}$ gene segments. Eight of the ten cDNA clones represent potentially functional messages, with the *V*, *D* and *J* elements joined in-frame. This may reflect the fact that a significant fraction of adult double negative cells express γδ receptors on their surface (5–10%)[9].

Four of the *V* sequences are identical (Z44, Z72, Z35 and Z14), indicating that this V_δ gene segment is expressed preferentially in adult double-negative thymocytes. V_δ sequences of DN4 (ref. 11) and Z10 are also identical. The V_δ nucleotide sequence of Z53 is similar (96%) to the Z49 sequence and the previously published V_δ sequence pλ12 (94%)[11]; the differences may reflect strain polymorphism (Fig. 1*b* legend). The V_δ sequence of clone Z80 is identical to that of Z49 except for a large central deletion which spans 134 nucleotides and results in a translational frame shift. Perhaps the Messenger RNA corresponding to Z80 arose from a transcript spliced using signal sequences within the *V*-region. The *V* region of Z68, which was found only once in these libraries, is virtually identical (99%) to the previously published V_α TA1 (ref. 13). Z78 (Fig. 1*a*) contains a VDJ junction which involves both the $D_{\delta1}$ and $D_{\delta2}$ gene segments.